Morphological Investigation of UV-Curable Polymer-Dispersed Liquid-Crystal (PDLC) Materials

Andrew J. Lovinger,* Karl R. Amundson, and Don D. Davis

AT&T Bell Laboratories, Murray Hill, New Jersey 07974

Received March 17, 1994. Revised Manuscript Received May 16, 1994[⊗]

We have examined the morphology of polymer-dispersed liquid-crystal materials (PDLCs), which show great potential for display applications. The materials were blends of a eutectic nematic liquid-crystal (LC) mixture and a UV-cross-linkable polymeric matrix and were examined in thin films. A variety of morphologies ranging from two-phase, polymer-dispersed LC droplets, to single-phase nematic spherulites was obtained depending upon composition and irradiation temperature. The effects of irradiation dose were also investigated. Scanning electron micrographs show that the LC drops depart significantly from sphericity and can have fused or satellite droplets, as well as bimodal size distributions in the 0.2−8-μm range. The spherulitic morphologies (which predominate following UV irradiation above 10 °C for 25% LC to above 65 °C for 60% LC) start from a central $s = +1$ disclination line and grow through accretion of LC molecules in a tangential orientation. Profuse radially oriented defects were identified as surface inversion walls; they appear to be initiated by factors both inherent to the spherulite and external (e.g., surface influences and local compositional variations). These inversion walls are consistently initiated at $s = +1/2$ disclination lines (and not at $s = -1/2$) and are reoriented parallel to the boundaries at the points of spherulitic impingement even though their local molecular orientation remains unchanged. They, as well as the overall spherulitic morphology survive heating above the nematic-to-isotropic transition (and subsequent cooling), with the exception of the regions near the interspherulitic boundaries, where some rearrangement of inversion-wall features is observed.

Introduction

Polymer-dispersed liquid crystals (PDLC) are becoming increasingly interesting as novel materials for display applications.[1] This is because they offer a number of potential advantages over the well-established nematic devices (twisted and supertwisted) as well as over a number of other competitors (e.g., ferroelectric or emissive): (1) They require no polarizers (which absorb more than half of the transmitted light), thus increasing brightness, minimizing heat-control problems, and reducing power and weight; (2) they require no alignment layers or stringent thickness control, thus greatly simplifying processing and enabling larger-size displays.

PDLCs have been described extensively in the literature (e.g., refs 1−5). They operate on the basis of a micrometer-sized dispersion of nematic liquid crystal (LC) droplets within a polymeric matrix. The liquid crystals have a positive dielectric anisotropy and therefore align with their director parallel to an electric field; they are selected so that their ordinary refractive index (n_0) matches the refractive index of the polymer matrix. Thus, the film is normally scattering because of random orientation of n_0 in the absence of an electric field but becomes transparent when such a field is applied, since LC alignment provides an effective refractive index that is the same for matrix and droplets.

Phase separation of PDLCs is accomplished (a) through solution casting of polymer and LC from a common solvent, (b) by cooling a thermoplastic/LC mixture below an upper-critical-solution temperature, or (c) by cross-linking a monomer or prepolymer within which the LC is soluble.[4] The latter case (cross-linking) can be effected thermally or optically. Among all of these methods, UV-initiated cross-linking is by far the most common one because of its use of low-viscosity materials and simple processing[4] and is therefore the subject of this investigation.

A number of parameters affect the electro-optic performance of PDLCs, of which droplet size and shape are paramount. These are determined primarily by composition, by cure rate and extent (which in turn are functions of UV light intensity and temperature), and by the mutual solubility of LC with the monomer, cross-linked polymer, and intermediate-stage oligomers and polymers. It is obvious that PDLCs are therefore very complex systems, which require precise morphological and processing control. Much understanding of their curing process and phase behavior has been obtained through the calorimetric studies by Smith.[6,7] As regards morphology, scanning electron micrographs of polymer/LC blends have been published, primarily for nematics dispersed in aqueous emulsions of poly(vinyl alcohol).[8−10]

[⊗] Abstract published in *Advance ACS Abstracts,* July 1, 1994.

(1) Doane, J. W. *Liquid Crystals: Applications and Uses*; Bahadur, B., Ed., World Scientific: River Edge, NJ; Vol. 1, Chapter 14.
(2) Doane, J. W.; Vaz, N. A.; Wu, B.-G.; Zumer, S. *Appl. Phys. Lett.* **1986**, *48*, 269.
(3) Vaz, N. A.; Smith, G. W.; Montgomery, G. P., Jr. *Mol. Cryst. Liq. Cryst.* **1987**, *146*, 1.
(4) West, J. L. *Mol. Cryst. Liq. Cryst.* **1988**, *157*, 427.
(5) Hirai, Y.; Niiyama, S.; Kumai, H.; Gunjima, T. *Rep. Res. Lab. Asahi Glass Co.* **1990**, *40*, 285.
(6) Smith, G. W. *Mol. Cryst. Liq. Cryst.* **1991**, *196*, 89.
(7) Smith, G. W. *Phys. Rev. Lett.* **1993**, *70*, 198.
(8) Drzaic, P. S. *Liq. Cryst.* **1988**, *3*, 1543.
(9) Drzaic, P. S.; Muller, A. *Liq. Cryst.* **1989**, *5*, 1467.

0897-4756/94/2806-1726$04.50/0

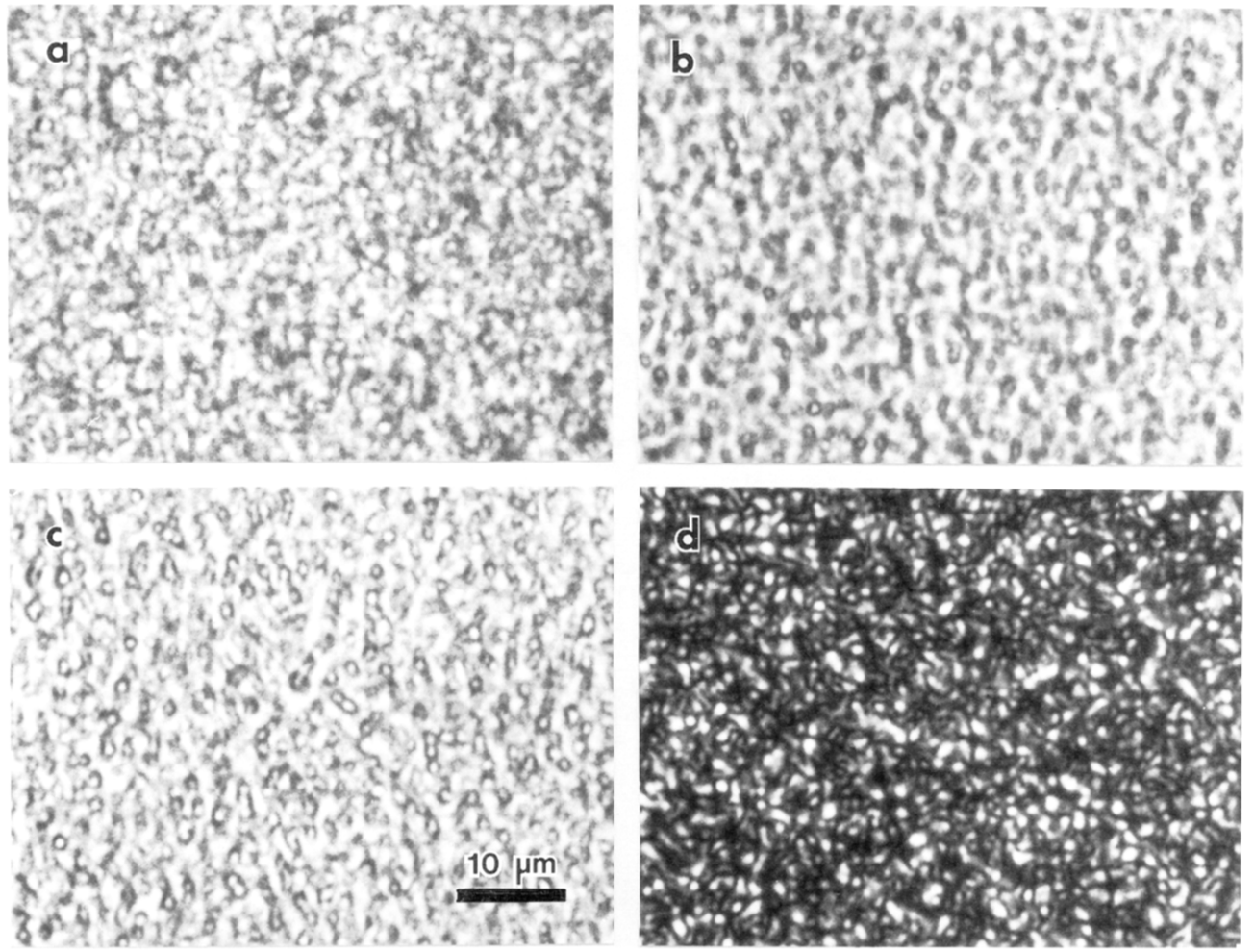

Figure 1. Optical micrographs (nonpolarized light) of 50:50 E7:NOA65 blends, UV-irradiated at 30 °C with doses of (a) 0.11 J/cm^2, (b) 0.45 J/cm^2, and (c) 13.50 J/cm^2. (d) Same as (c) but between crossed polars.

However, we are not aware of detailed studies of PDLC morphology as a function of composition, UV dose, and temperature. It is the purpose of this paper to provide such morphological understanding for a very typical and most commonly used polymer/liquid-crystal system.

Experimental Section

The liquid-crystal component used was a eutectic mixture from BDH Merck Industrial Chemicals, Poole, England. It is designated E7, has a nematic-to-isotropic transition at 59–60 °C, a smectic-to-nematic transition below −20 °C, and consists of 51% *n*-pentylcyanobiphenyl, 25% *n*-heptylcyanobiphenyl, 16% *n*-octyloxycyanobiphenyl, and 8% *n*-pentylcyanoterphenyl.[11] The matrix was a photopolymerizable mixture designated NOA65 and manufactured by Norland Products, Inc., New Brunswick, NJ. It is reported by Smith[6] to comprise primarily trimethylpropane diallyl ether, trimethylolpropane tristhiol, isophorone diisocyanate ester, and benzophenone photoinitiator. The manufacturer reports[12] that this material has a refractive index of 1.524 and a maximum optical absorption in the 350–380-nm range (being essentially transparent above 420 nm).

The materials were stored in the dark and handled in the absence of sunlight and under diminished room lights to eliminate any unwanted photopolymerization or phase separation; in control experiments, initiation of phase separation required over 3 h under these conditions. The PDLCs were prepared by irradiation of predetermined mixtures of NOA65 and E7 using a 100-W Hg lamp (Blak-ray, UVP Inc., San Gabriel, CA) which provides ca. 7.5 mW/cm^2 of ultraviolet radiation with a peak at 365 nm. The irradiation dose was measured with a Newport Optical Power Meter equipped with UV silicon detector. The blended samples had been sandwiched between glass cover slips and confined to thicknesses of 12–18 μm using glass-bead spacers. The temperature of photopolymerization and phase separation was controlled to ±0.5 °C with the thermal stage of a Mettler FP82 microscope oven whose cover had been kept open and which had been calibrated with thermometric standards. Sample morphologies were recorded in a variety of optical microscopes and in a JEOL 100-CX electron microscope operated in the scanning mode and using a secondary electron detector.

Results and Discussion

The typical morphology of PDLCs consists of LC-rich droplets distributed within a polymer-rich matrix. Such morphology is seen in Figure 1 following various UV doses for a 50:50 LC:polymer blend irradiated at ambient temperature. It is remarkable that phase separation occurs extensively even at very low doses, as seen in Figure 1a (0.11 J/cm^2, corresponding to a 15-s irradiation). The droplets are ca. 1–4 μm in diameter, although exact determination is difficult because of multiple overlaps across the film thickness. Equally remarkably, there appears to be no substantial change in PDLC morphology at this level of resolution following

(10) Havens, J. R.; Leong, D. B.; Reimer, K. B. *Mol. Cryst. Liq. Cryst.* **1990**, *178*, 89.
(11) Zhong, Z. Z.; Schuele, D. E.; Gordon, W. L.; Adamic, K. J.; Atkins, R. B. *J. Polym. Sci., Polym. Phys. Ed.* **1992**, *30*, 1443.
(12) Technical Data Sheet for Norland Optical Adhesive 65, Norland Products Inc., New Brunswick, NJ.

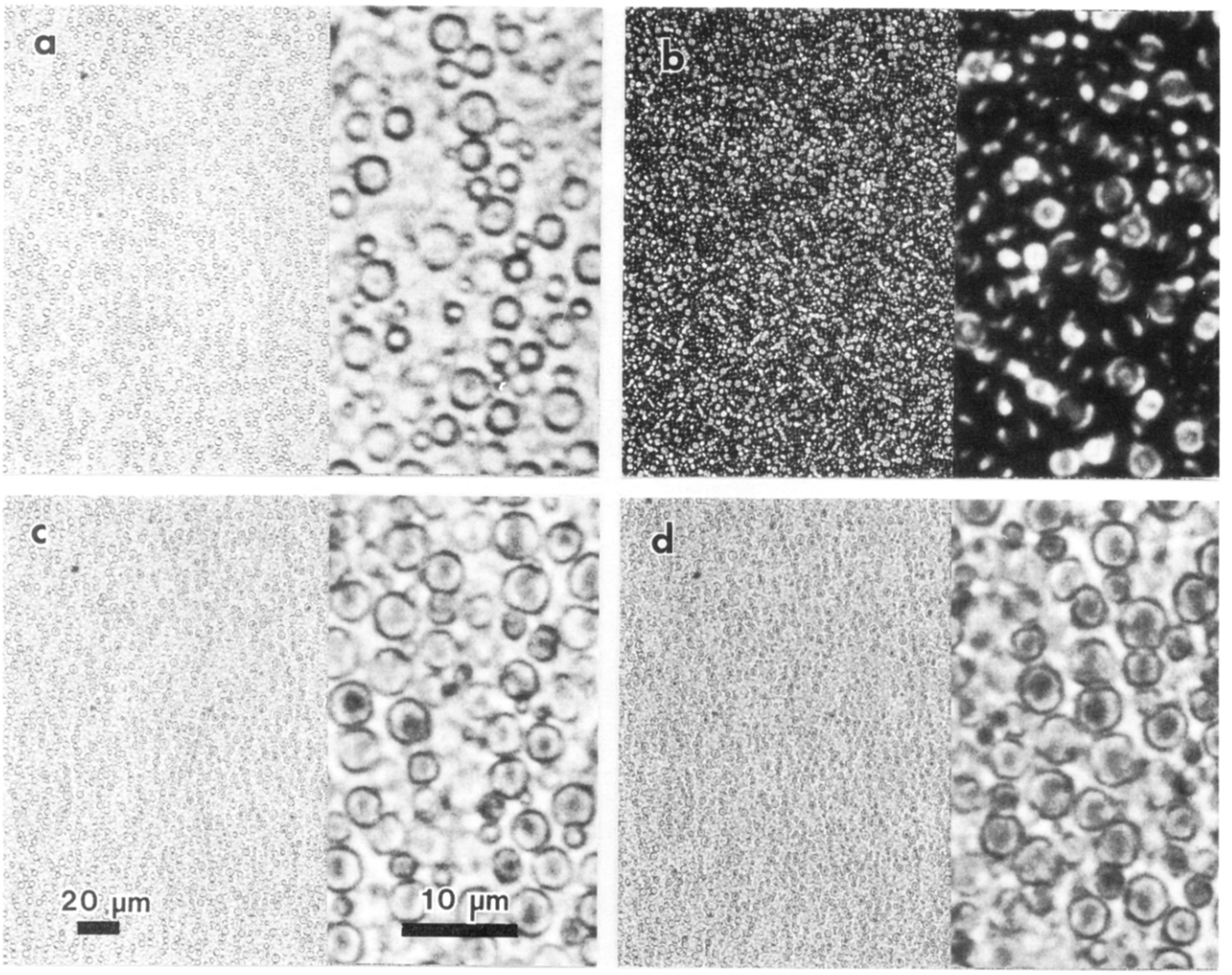

Figure 2. Morphology of minimally cured 50:50 E7:NOA65 blends following a UV dose of 0.04 J/cm^2 at 30 °C: (a) immediately after irradiation; (b) 2 min, (c) 11 min, and (d) 30 min after irradiation. All are optical micrographs using transmitted nonpolarized illumination except (b), which is with crossed polars.

much higher UV doses (e.g., 13.50 J/cm^2, corresponding to 30 min of irradiation: Figure 1c,d). This suggests [in agreement also with other studies[13,14]] that phase separation and droplet nucleation occurs very early in the photopolymerization process, and that further cure serves primarily to cross-link extensively an already well-separated matrix within which further droplet generation is uncommon (except perhaps at length scales below the limit of optical resolution, as is discussed later in connection with Figure 3). This also agrees with DSC studies of PDLC cure,[6] which report that more than half of the LC is retained within the polymeric matrix in the same PDLC system as ours even after extensive cure (the maximum degree of cure in the PDLC was ca. 93% of the maximal value for pure NOA65).[6]

In fact, the initial phase separation is even more rapid than inferred from Figure 1a. We have been able to induce it even after a 0.04 J/cm^2 dose (5 s under our experimental conditions) and to study the temporal evolution of the morphology after initial droplet nucleation and in the absence of significant further photopolymerization. As seen in Figure 2a, the morphology of a 50:50 LC:polymer system immediately after a 5-s irradiation consists already of extensively dispersed liquid-crystal droplets, which have unusually regular and well-defined spherical shapes with a diameter of ca. 2−4 μm. Their high spherical uniformity is presumably the result of two major factors: (a) the minimal degree of polymerization, which preserves the matrix in a liquid state and thus allows interfacial tension to impart sphericity unencumbered by mechanical stresses; (b) the incipience of phase separation, which has not yet led to severe droplet collisions and consequent distortions and fusion.

Two minutes after UV irradiation (Figure 2b) the number density of droplets is seen to have increased, with many more droplets of a size ≤ 1 μm but without a detectable increase in the size of the larger droplets. These observations demonstrate that phase separation, once initiated, *is continuing even in the absence of further photopolymerization*. Moreover, they imply that the mechanism of this phase separation is primarily nucleation-based (i.e., the growth rate of existing droplets is much lower than the rate of nucleation).

Further phase separation is seen in Figure 2c (11 min) and 2d (30 min after the UV exposure). The nucleation of new LC droplets continues to be dominant, while their

(13) Montgomery, G. P.; Vaz, N. A.; Smith, G. W. *Proc. SPIE* **1988**, *958*, 104.
(14) Lackner, A. M.; Margerum, J. D.; Ramos, E.; Lim, K. C. *Proc. SPIE* **1989**, *1080*, 53.

growth remains restricted. From the mean sizes at 5 s, 2 min, and 11 min, we estimate this growth rate to be an average of 0.11 μm/min during this time interval, although we do not expect it to be linear. This rate is to be contrasted with the mean growth rate during the 5 s of photopolymerization (ca. 22.2 μm/min). Another contrast is with the growth *beyond* 11 min, which is now seen (Figure 2d) to be severely restricted. In essence, the smaller droplets grow to the maximal size of the preexisting ones, i.e., 3.5–5 μm, which *does not increase further*. From Figure 2d it is apparent that this restriction arises from space-filling considerations which are also responsible for the pronounced deviations from perfect sphericity of the individual droplets (especially at impact boundaries). The droplet-size uniformity achieved in this manner is unusual and may be desirable for some device applications. Our findings suggest that a three-stage process of (a) extensive droplet nucleation by a very small UV dose, followed by (b) growth to fairly uniform sizes in the absence of irradiation, and (c) freezing-in by a subsequent brief, high-dose exposure, might produce well-controlled and advantageous PDLC morphologies.

The morphology of the droplets following a more typical processing treatment that leads to "full" cure[6,7,12] (4.5 J/cm^2) is seen at higher resolution in the scanning electron micrographs of Figure 3 (which are similar to those from LC/polymer emulsions[8–10]). Here the liquid crystal droplets have been extracted with carbon tetrachloride. The bright regions at the droplet peripheries are artifacts of the topography (edge effects leading to excess production and detection of secondary electrons). There is a wide distribution of cavity sizes covering the range 0.2–8 μm, which appears clearly bimodal. Very interestingly, most of the large cavities are seen at the high magnification of Figure 3b to have at their peripheries very small "satellite" droplets that were not detectable in the optical microscope. These "satellite droplets" have nucleated at the interstices between the larger ones, presumably at the latter stages of phase separation. There is widespread evidence in this figure for intersection and fusion of individual LC drops leading to large agglomerates with highly irregular boundaries. Micrographs such as that of Figure 3b demonstrate how far the ultimate droplet morphology actually is from the usual assumption of sphericity.

In the remainder of this paper we now examine the effects of composition and cure temperature on PDLC morphology. Both of these parameters are of central importance in use of these materials for display devices. As regards composition, it has been reported for a different PDLC system[5] that LC contents of >55% are optimal for light-shutter applications. With regard to temperature, the greatest degree of cure and of phase separation has been found[6] to occur around 55 °C.

Figure 4 depicts optical micrographs for a 65:35 E7:NOA65 blend subjected to "full cure" (4.5 J/cm^2 corresponding to a 10-min irradiation) at various temperatures. In all cases we found extensive phase separation in the typical manner of PDLCs i.e., LC-rich droplets frozen into a cross-linked polymer-rich matrix; this agrees with the findings of Hirai et al.[5] for a ternary system of LC, monomer, and oligomer. In our case, the droplet sizes decrease from 5–6 μm as the polymerization temperature is raised from ambient to 40 °C (Figure 4a,b); further increase to 60 °C (Figure 4c) seems to have no additional effect. Such a decrease in size is consistent with maximal phase separation and degree of cure,[6] which, as we saw earlier, tends to occur through increased nucleation of new droplets rather than growth of existing ones.

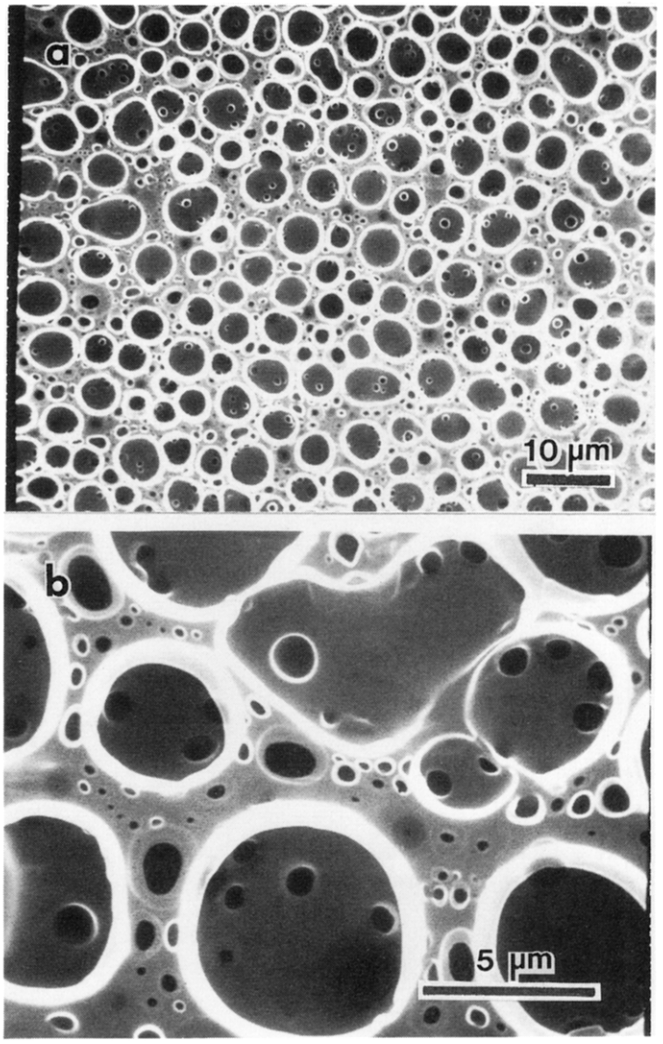

Figure 3. Morphology of a 50:50 E7:NOA65 blend after UV curing with 4.5 J/cm^2 at 30 °C and extraction of the liquid-crystal phase. Scanning electron micrograph, secondary electrons.

Most of the previous studies of PDLCs have been performed on 50:50 blends. The characteristic morphology of such blends of E7:NOA65 is seen in Figure 5 for four different temperatures of photopolymerization. The expected droplet dispersion is obtained through 40 °C. However, from a temperature of 45 °C or higher, a radically different morphology is observed, which resembles strongly the spherulitic or axialitic one that typifies semicrystalline polymers (see, e.g., refs 12–14). 40–45 °C actually represents a transition between these two morphological régimes, as droplet dispersions are observed admixed with the spherulitic-like morphology. It is seen in Figure 5c that these spherulites are fully space-filling and that therefore there is either no phase separation between polymer and liquid crystal (i.e., growth involves a mixed phase), or, if there is, it must consist of the *reverse* of typical PDLCs, i.e., of small polymeric regions dispersed within these very large (millimeter-sized!), birefringent liquid-crystalline entities. Further detail about this spherulitic-like morphol-

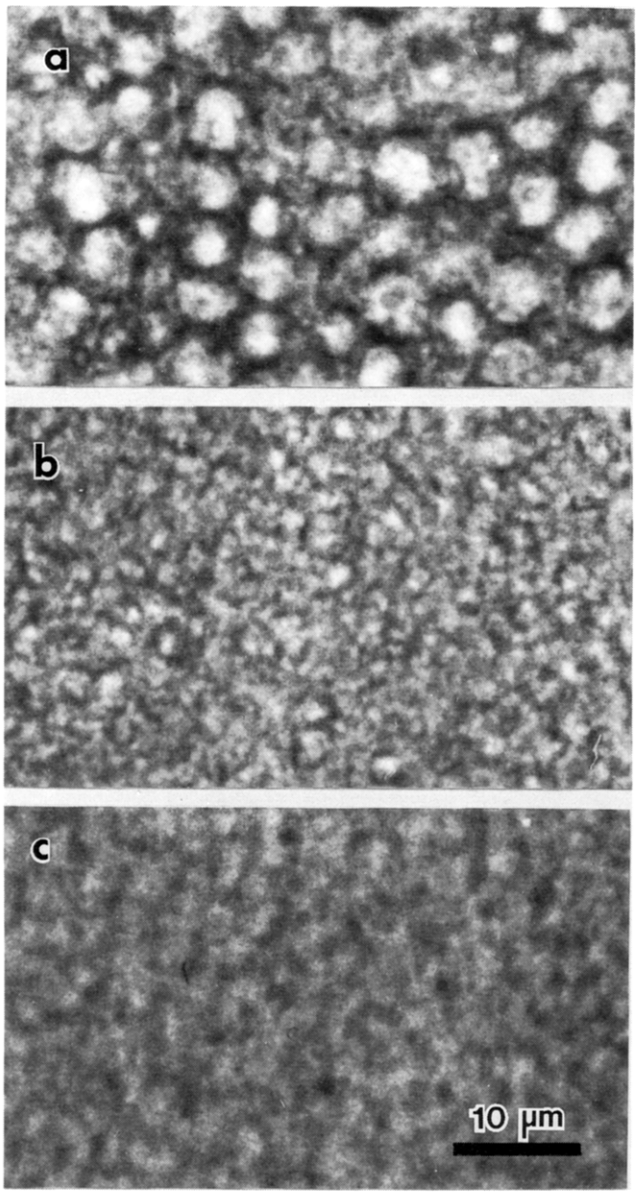

Figure 4. Morphology of a 65:35 E7:NOA65 blend UV-cured with 4.5 J/cm^2 at (a) 30, (b) 40, and (c) 60 °C. Transmitted, nonpolarized illumination.

ogy will be given later after discussion of its compositional and temperature dependence.

For a 35:65 E7:NOA65 mixture, the typical PDLC droplet morphology is obtained only near room temperature (Figure 6a). Photopolymerization at 40 °C or above yields the spherulitic-like morphology (Figure 6b); both morphologies coexist around 30–35 °C. These entities are once again space-filling (as for the 50:50 composition) and more regular in their growth features, implying greater uniformity of growth than for their more LC-rich counterparts (e.g., Figure 5c).

As the blend composition becomes richer in polymer (e.g., 25:75 E7:NOA65) the PDLC droplet morphology is no longer attainable without cooling. Typical spherulitic morphologies are obtained for temperatures between 30 and 70 °C (see Figure 7a,b), with no systematic differences as a function of temperature; droplet-type morphologies were obtained only by cooling to 10–15 °C, but transformed to macroscopic nematic structures at ambient temperatures (Figure 7c). From these compositional studies we see that transition temperatures between PDLC-type morphologies (formed at low temperatures) and spherulitic morphologies (formed at high temperatures) increase rapidly with LC content over a fairly narrow range (see Figure 8). Beyond ca. 70% E7 the two components (prepolymer and liquid crystal) are no longer mutually soluble, so that macroscopic phase separation is obtained even without irradiation. At the other compositional side (i.e., below ca. 30% E7 at room temperature) the liquid crystal and polymer remain mutually soluble, so that instead of phase separating as droplets, the liquid-crystal molecules associate into the nematic phase from what is now a very viscous solution (because of the large amount of polymer). Growth from viscous environments is well known to be the main factor promoting crystallization into spherulitic morphologies in semicrystalline polymers, as well as in organic and inorganic materials.[15–17] As the E7 content drops below ca. 20%, there is no longer sufficient liquid crystal to form space-filling structures, so that only isolated spherulites are obtained. Close to the pure components, single phases of each are seen in the optical microscope. Any phase separation that may occur upon irradiation is probably at a very fine scale.

At this point, we can examine the detailed morphological characteristics of these LC/polymer "spherulites". These entities are not spherulites in the strictest sense, since they do not have three-dimensional spherical symmetry. In their films and at some distance from the nucleus, even the ubiquitous spherulites of semicrystalline polymers are in essence "cylindrulites" (see Figure 9a). The structure of the central core depends upon whether nucleation is homogeneous or heterogeneous, and in the latter case whether it occurs on the substrate surfaces or in the interior of the thin film (a homogeneous nucleus occurring in the interior is depicted in Figure 9a). For nematic liquid crystals, two possibilities can be envisioned: a disclination line whose ends are anchored at the two surfaces (Figure 9b) or an escaped disclination into the third dimension leading to a point singularity that is attached to one of the surfaces[18,19] (Figure 9c). For a thin film, an $s = +1$ disclination line with ends attached to the glass surfaces should be stable (contrary to such disclination lines in the bulk).[20] The fact that circular interference fringes are not observed around the core also argues for a stable disclination line.

The next important point to be made about these spherulites is their molecular orientation. The Maltese crosses rotate in the same sense and rate as the crossed polars, confirming the $s = +1$ assignment. Using a first-order red plate, we determined that the spherulites are *negatively* birefringent (the retardation in the first and third quadrants decreases to first-order yellow and in the others increases to second-order blue). This implies that the molecules are oriented *tangentially* (see Figure 10), since the extraordinary refractive index (corre-

(15) Keith, H. D.; Padden, F. J. *J. Appl. Phys.* **1963**, *34*, 2409; **1965**, *35*, 1270, 1286.
(16) Geil, P. H. *Polymer Single Crystals*, Wiley: New York, 1963.
(17) Wunderlich, B. *Macromolecular Physics*; Academic: New York, 1973; Vol. 1.
(18) Demus, D.; Richter, L. *Textures of Liquid Crystals*; Brown, G. H., Ed.; Academic: New York, 1975; Vol. 1.
(19) Kléman, M. In *Advances in Liquid Crystals*; Brown, G. H., Ed.; Academic: New York, 1975; vol. 1.
(20) Cladis, P. E., private communication.

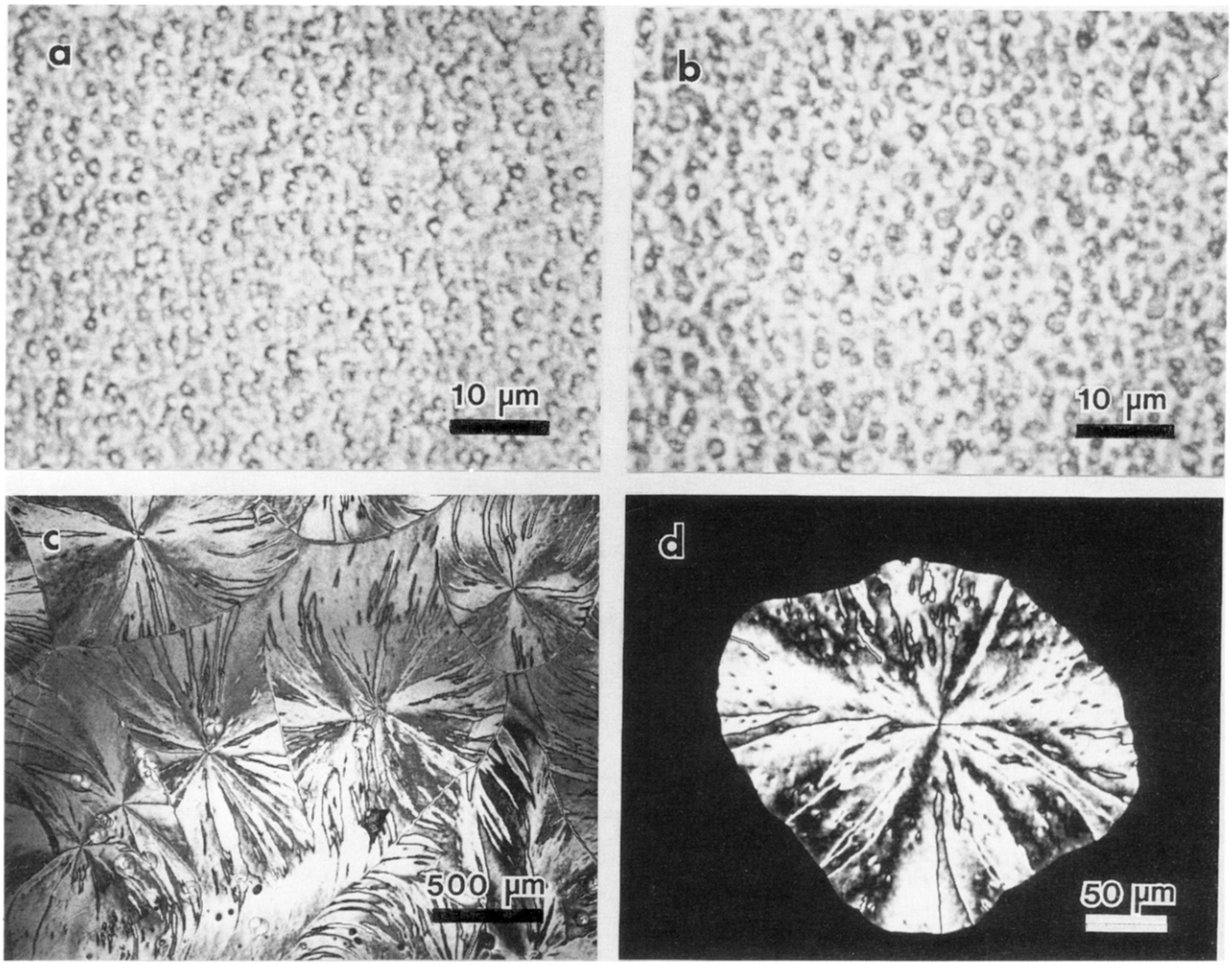

Figure 5. Morphology of a 50:50 E7:NOA65 blend UV-cured with 4.5 J/cm^2 at (a) 30, (b) 40, (c) 50, and (d) 60 °C. (a, and b) Nonpolarized illumination, (c and d) sample between crossed polars.

sponding to the nematic director) is larger than the ordinary ($n_e = 1.7$, $n_o = 1.5$ for E7). Such tangential orientations are almost universal in polymeric spherulites (Figure 11a), where their origin is now well understood:[15-17] it arises from the crystallization of polymers in the form of thin platelets (lamellae) emanating from a central nucleus and having their molecular stems generally folded normal to the lamellar surfaces. However, in the LC/polymer case the exact arrangement of individual rigid rods into "lamellar" or other ordered structures is not known, although our optical evidence is consistent with an arrangement of the type depicted schematically in Figure 11b. Both thermodynamic and kinetic factors would favor growth of LC molecules that attach themselves parallel to an established growth substrate (front). A likely reason is thermodynamic. From consideration of entropy the tangential orientation of the nematic director is preferred at interfaces in the absence of overwhelming anisotropic enthalpic interactions. Since the rigid rods have to accrete through a viscous, partly cross-linked polymer matrix, the overall growth of the resulting spherulite will be maximized if these localized fronts become radial; space-filling considerations will also promote growth of those fronts that have been oriented radially. Therefore, even in the absence of lamellar morphologies, we speculate that tangential molecular orientation should be preferred. In addition, surface alignment will also tend to keep these rods parallel to the glass substrates (except perhaps at the core), thus imposing an additional restriction on their three-dimensional orientation.

A most striking morphological feature of these LC/polymer spherulites is the radial striations that are exhibited by all of them to varying degrees. The spectrum of typical behavior is already evident in Figure 7a,b. The large spherulite in Figure 7a represents one end of that spectrum (containing only very few such striations), while the central spherulite in Figure 7b represents the other (being essentially covered by these); the remaining entities in these figures show the more common, intermediate, morphology. Between crossed polars these entities generally exhibit *closed loops*, with the material inside the loop having opposite birefringence to that outside. They therefore represent *surface inversion walls*[21,22] that are anchored to the two glass substrates. Their ends are $s \pm 1/2$ disclination lines normal to these surfaces (see the schematic drawings of Figure 12). The inversion walls are occasionally *not closed*, leading to diverging sectors (as in the lower-right spherulite of Figure 7b) and gross disruption of the Maltese-cross pattern. In some spherulites this Maltese cross is oriented at ±45° with respect to the polarizer and analyzer (instead of the much more common paral-

(21) Nehring, J.; Saupe, A. *J. Chem. Soc., Faraday Trans. 2* **1972**, *68*, 1.
(22) Kléman, M.; Williams, C. *Philos. Mag.* **1973**, *28*, 725.

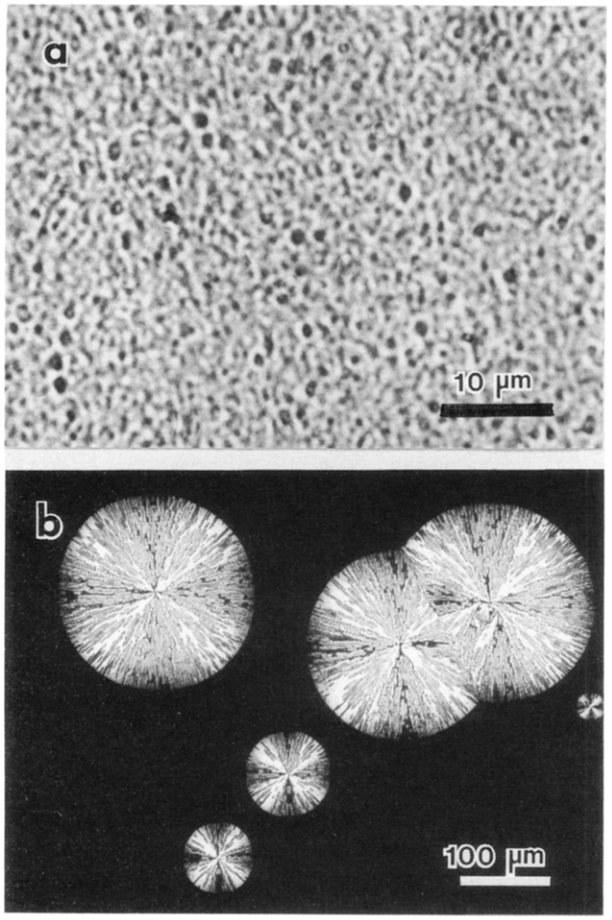

Figure 6. Morphology of a 35:65 E7:NOA65 blend UV-cured with 4.5 J/cm^2 at (a) 30 and (b) 40 °C: (a) nonpolarized illumination, (b) sample between crossed polars.

lel orientation), indicating a spiraling molecular arrangement as depicted schematically in Figure 10b.

Two possible types of inversion wall are shown in Figure 12a,b: the defect may start at an $s = +1/2$ disclination and end at an $s = -1/2$ as the spherulitie grows outward, or vice versa. We can determine which of these two possibilities is the operative one by examining the changes in the extinction features of these inversion walls as they are rotated between fixed cross polars. As seen in Figure 13, the two dark brushes of each of the four numbered defects are of equal width when it is located at $n\pi/4$ positions with respect to the polars. However, at all other positions the brush closest to a polar narrows slightly while the outer one widens broadly. By reexamining the schematics of Figure 12 in light of this behavior, we see that only the model of Figure 12a is consistent with our optical findings. It is remarkable that this conclusion holds for *all* inversion wall defects that we examined in many spherulites.

Reasons for this propensity of inversion walls to be initiated exclusively by $s = +1/2$ defects in spherulitic growth are not certain. One possible explanation is that, in the opposite case (Figure 12b), the molecules in the defective orientation would be ahead of the spherulitic growth front and would thus propagate freely unless some fortuitously localized interruption in their accretion allowed the rest of the spherulitic front to "catch up". On the other hand, the observed situation (Figure 12a) could arise simply by a perturbation at any point of the spherulitic front causing localized retarda-

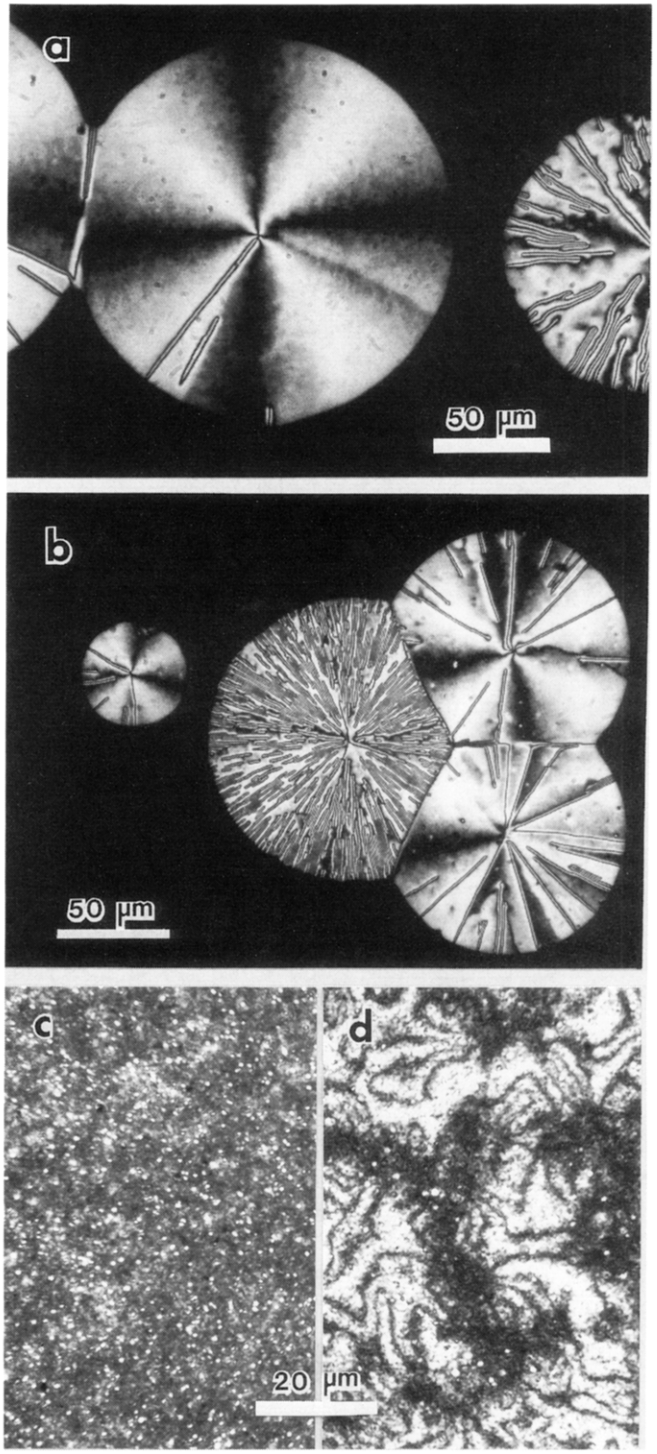

Figure 7. Morphology of a 25:75 E7:NOA65 blend UV-cured with 4.5 J/cm^2 at (a) 30, (b) 40, and (c) 10 °C, as recorded in the polarizing microscope. (d) The same area as in (c) after 10 min at ambient temperature.

tion of growth. Such a perturbation might be a packet of polymer molecules, e.g., a region of denser cross-linking or entanglement. It could, in principle, be any other heterogeneity (for example, the glass microscope spacers), but the profusion of inversion walls would not be consistent with this. Then the operative distinction between initiating positive vs negative disclinations would depend upon the relative wetting of the isotropic vs nematic phases onto the surfaces of the defect (see Figure 14). If the nematic phase has a greater affinity toward the polymer surface than does the isotropic, tangential anchoring will occur leading to an $s = -1/2$

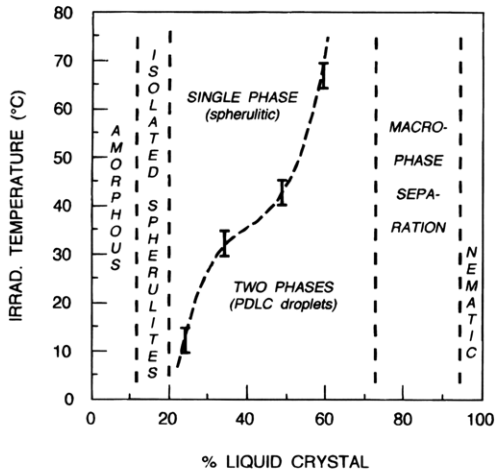

Figure 8. Phase diagram of E7:NOA65 as a function of composition and irradiation temperature.

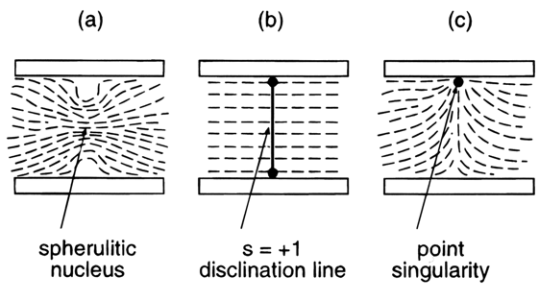

Figure 9. Schematic diagrams comparing the central regions of (a) crystalline polymer spherulites vs (b) and (c) nematic LC spherulites, for thin-film growth between two flat surfaces.

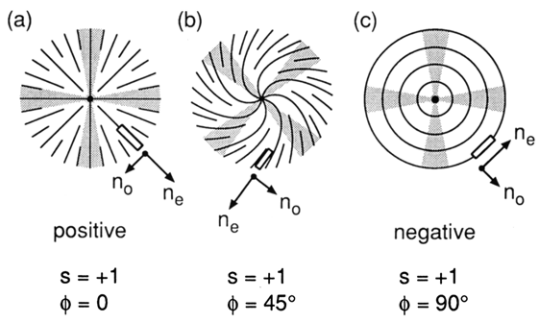

Figure 10. Schematic diagrams of nematic LC spherulites growing around a central $s = +1$ disclination and having a molecular orientation ϕ with respect to the spherulitic radius. n_o and n_e are the directions of the ordinary and extraordinary refractive indices.

defect (Figure 14b); otherwise, the nematic front will advance around this defect, as depicted schematically in Figure 14a. Separate evidence from biphasic (nematic/isotropic) LC droplets dispersed within a polymer matrix[23] suggests that the latter is indeed the case.

A number of characteristics of these inversion walls are most noteworthy and can be summarized through Figures 7b and 15. First of all, their growth is initiated by *both* inherent and external factors. Figure 7b demonstrates the *inherent* influences as reflected in the cluster of three spherulites that have been nucleated adjacently and simultaneously (the latter is evidenced by the straight boundaries). Even though these three therefore have exactly the same thermal and UV-irradiation histories, as well as the same glass surface

(23) Amundson, K. R., unpublished results.

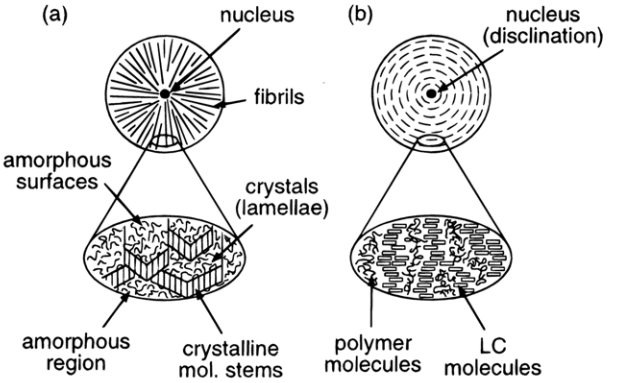

Figure 11. (a) Schematic model of the microstructure of typical polymer spherulites. (b) Possible hypothetical model for the microstructure of our nematic-LC/amorphous-polymer spherulites.

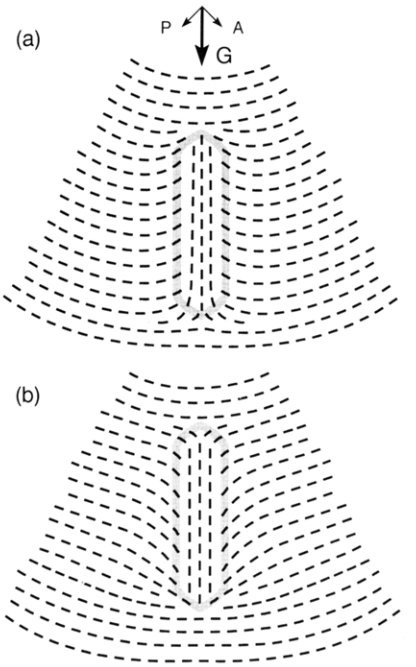

Figure 12. Schematic models of possible surface inversion walls in nematic-LC/amorphous-polymer spherulites. (a) Initiation at an $s = +1/2$ disclination line, (b) initiation at an $s = -1/2$ disclination line. A and P indicate the analyzer and polarizer directions, and G is the growth direction of the spherulite.

and nutrient environments, one is profusely dominated by such inversion walls while the others show a much sparser morphology. In polymeric spherulites, such drastic differences commonly result from polymorphism (e.g., in α- and β-isotactic polypropylene[24,25]) or change in crystallographic growth face (as in the even−even polyamides[26,27]). In the present LC case neither of these two mechanisms can be operative, yet the profusion of inversion walls in the central spherulite or Figure 7b implies an *inherent* tendency that is *propagated* outward from the nucleus. We should note that not only initiation but also *termination* of these defects is much more frequent here, contrary to the more general case

(24) Keith, H. D.; Padden, F. J., Jr.; Kissell, W. J.; Wyckoff, H. W. *J. Appl. Phys.* **1959**, *30*, 1485.
(25) Lovinger, A. J.; Chua, J. O.; Gryte, C. C. *J. Polym. Sci., Polym. Phys. Ed.* **1977**, *15*, 641.
(26) Khoury, F. *J. Polym. Sci.* **1958**, *33*, 389.
(27) Lovinger, A. J. *J. Appl. Phys.* **1978**, *49*, 5003, 5014.

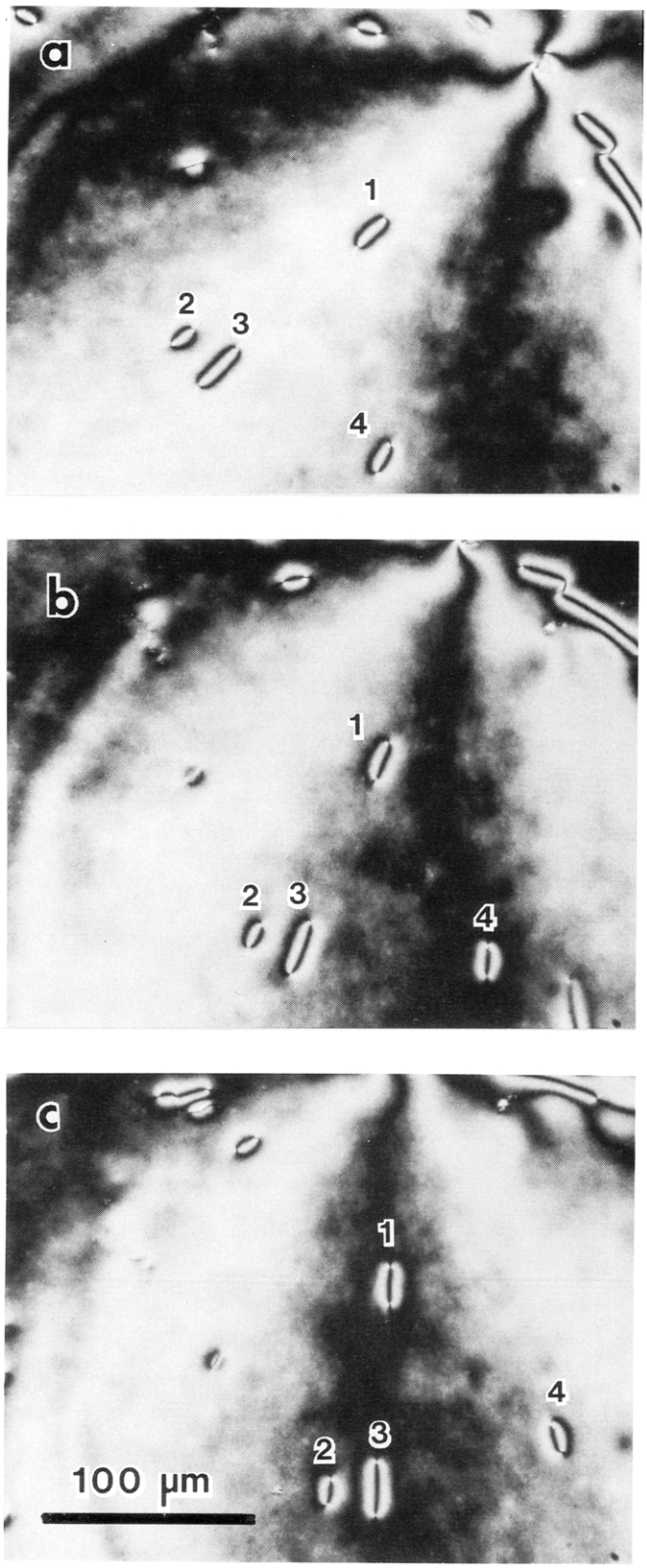

Figure 13. Polarizing optical micrographs from a portion of a 35:65 E7:NOA65 spherulite used to test the two models of Figure *12*. The specimen has been rotated so that defects 1 and 3 are at (a) 45° from the direction of the vertical polarizer, (b) 20° from it, and (c) parallel to it. Note the changing appearance of the inner vs outer brushes in the four numbered loops (see text).

where defects tend to propagate to the periphery. Perhaps local stress fields in the matrix network associated with the nucleation of particular spherulites persist during its growth and lead to frequent initiation

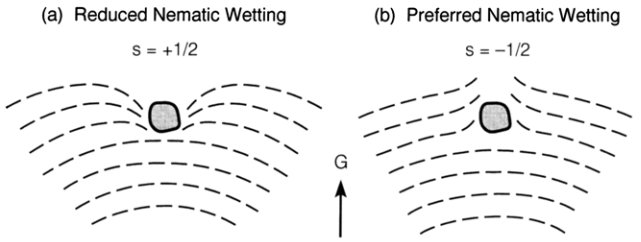

Figure 14. Schematic models for initiation of $s = +1/2$ defects on a hypothetical impurity (e.g., a cross-linked polymer region) depending upon preferred wetting of (a) the isotropic phase or (b) the nematic phase. G is the spherulitic growth direction.

and termination of defects.

Other phenomena associated with these inversion walls are summarized in Figure 15. These structures grow after completion of irradiation and cooling to well below the nematic−isotropic transition temperature (T_{ni}). Similar morphologies have also been obtained for specimens irradiated at room temperature . Figure 15a demonstrates the case of defects that do not originate at the nucleus, but, once initiated, cause a profusion of further inversion walls to be generated adjacently and even to bifurcate. The latter implies a *succession* of $s = +1/2$ disclinations and leads to the zigzag or crankshaft appearance of some of the extinguished regions. Figure 15b demonstrates convincingly the coexistence of *extrinsic* origins of the inversion walls: a line diagonally intersecting the spherulite is seen to have nucleated a profusion of inversion walls at the top, extending to a fraction of a mm and indifferent to local molecular orientation. A similar line is also recognizable in Figure 15a. Macroscopic inhomogeneities on the inner glass or ITO surfaces (e.g., minute scratches or cracks on the coating) are considered responsible for this mode of nucleation of inversion walls.

Figure 15c depicts the behavior of these surface inversion walls at common spherulitic boundaries. It is seen that these defects are not quenched but persist and are instead reoriented along the boundary. Remarkably, even though the walls are reoriented, the LC molecules in the core are *not* (as confirmed by the uniformity of the retardation color within the enclosed regions upon insertion of a first-order red plate). Thus, in the absence of a terminating event ($s = -1/2$ disclination) the molecules within these surface inversion walls retain their orientations and mode of growth even as they are redirected macroscopically by the pincer-like movement of the two colliding spherulites.

Finally, Figure 15d depicts the typical morphology within regions of "confined" isotropic phase (i.e., enclosed by previously grown nematic LC/polymer spherulites). The spherulites grown within these confined regions are always replete with inversion walls, which themselves are no longer radially directed but generally curved. The agglomerates formed by these loops are separated by channels of nematic material containing no such defects; the channels define a characteristic length scale corresponding to the width of 3−8 such surface inversion wall loops. This entire phenomenology is fully typical of growth of crystalline polymers in "impure" melts (i.e., those containing large amounts of noncrystallizable molecules, which tend to get rejected to the sides of the crystalline aggregates, thus forming the observed channels).[15] The occurrence of similar morphologies in the case of LC/polymer mixtures con-

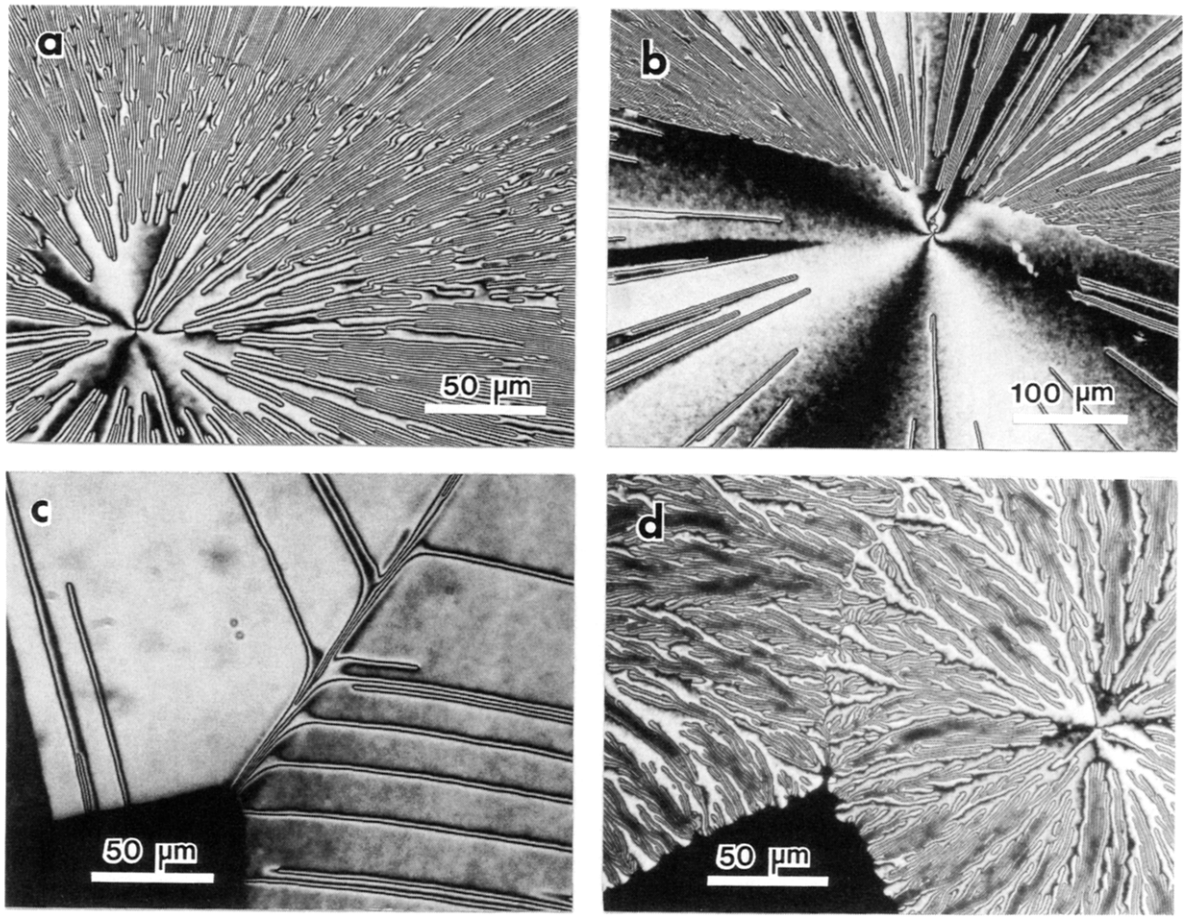

Figure 15. Morphological details of the characteristic surface inversion walls in 25:75 E7:NOA65 specimens UV-irradiated with 4.5 J/cm^2 at 70 °C (a–c) or 60 °C (d). (a) Successive radial initiation of such defects; (b) initiation by external inhomogeneities; (c) reorientation of such defects at interspherulitic boundaries; (d) growth in confined regions.

fined to enclosed regions suggests similar origins, i.e., enrichment of these regions with partly cross-linked polymeric molecules that have accumulated by rejection from the surrounding material, thus hindering aggregation of the LC molecules. The profuse generation of inversion walls in all spherulites at such regions, the macroscopic roughness of the growth interface, as well as an observed reduction in growth rate are all consistent with this interpretation.

The nematic–isotropic transition behavior of the spherulites supports these interpretations, as seen in Figure 16. Upon heating, the isotropic phase first appears within nucleation sites at temperatures very close to T_{ni} of pure E7. The nucleation sites proliferate in areas of high inversion-wall density and are most prevalent along the outer regions of the spherulites rather than near their centers. Both of these observations support the interpretation that inversion walls are initiated by impurities such as regions of high polymer concentration and that impurities are partially rejected at the growth front. Individual spherulites "melt" at slightly different temperatures, which correlate loosely with the density of inversion-wall defects. After the film is heated at 65 °C (at which the sample is completely isotropic) and then cooled back down even after times as long as 165 min, the spherulites reappear in almost exactly the same form, including the arrangement of inversion walls (see Figure 16d). Similar results were also obtained for samples heated to higher temperatures (70 °C) but only for brief periods of a few minutes. After such treatment, the originally radial inversion walls near the edges of the spherulites become more irregular and curved (as in Figure 16d). This shows that elements external to the nematic phase (e.g., surface forces, polymer network) are centrally related to the observed defect structure. In fact we have found that an "imprint" of the spherulitic outline is preserved by the polymer network even at very high temperatures (90 °C). The fact that the memory of inversion-wall textures is less long-lived near the interspherulitic boundaries implies changes in the growth environment along the spherulitic radius that lead to cumulative effects in a manner analogous to the rejection phemomena characterizing growth of crystalline polymers.[15]

Conclusions

Our study has shown that this typical PDLC material (E7/NOA65) can exhibit a variety of morphologies depending upon composition and irradiation temperature. Microdroplet dispersions are obtained at temperatures ranging below ca. 15 °C for a 25% E7 mixture to 70 °C for a 60–65% liquid-crystal content. Above these irradiation temperatures very unusual spherulitic-type morphologies are obtained. The PDLC morphology induced in the 25% LC blend is not stable at room temperature but transforms partly to a continuous nematic. The morphological uniformity of PDLC droplets is highest for the 65% LC blend, for which the typical sizes decrease from ca. 5 to 1 μm by increasing the temperature during cure. Nevertheless, scanning electron microscopic examination of cavities from which

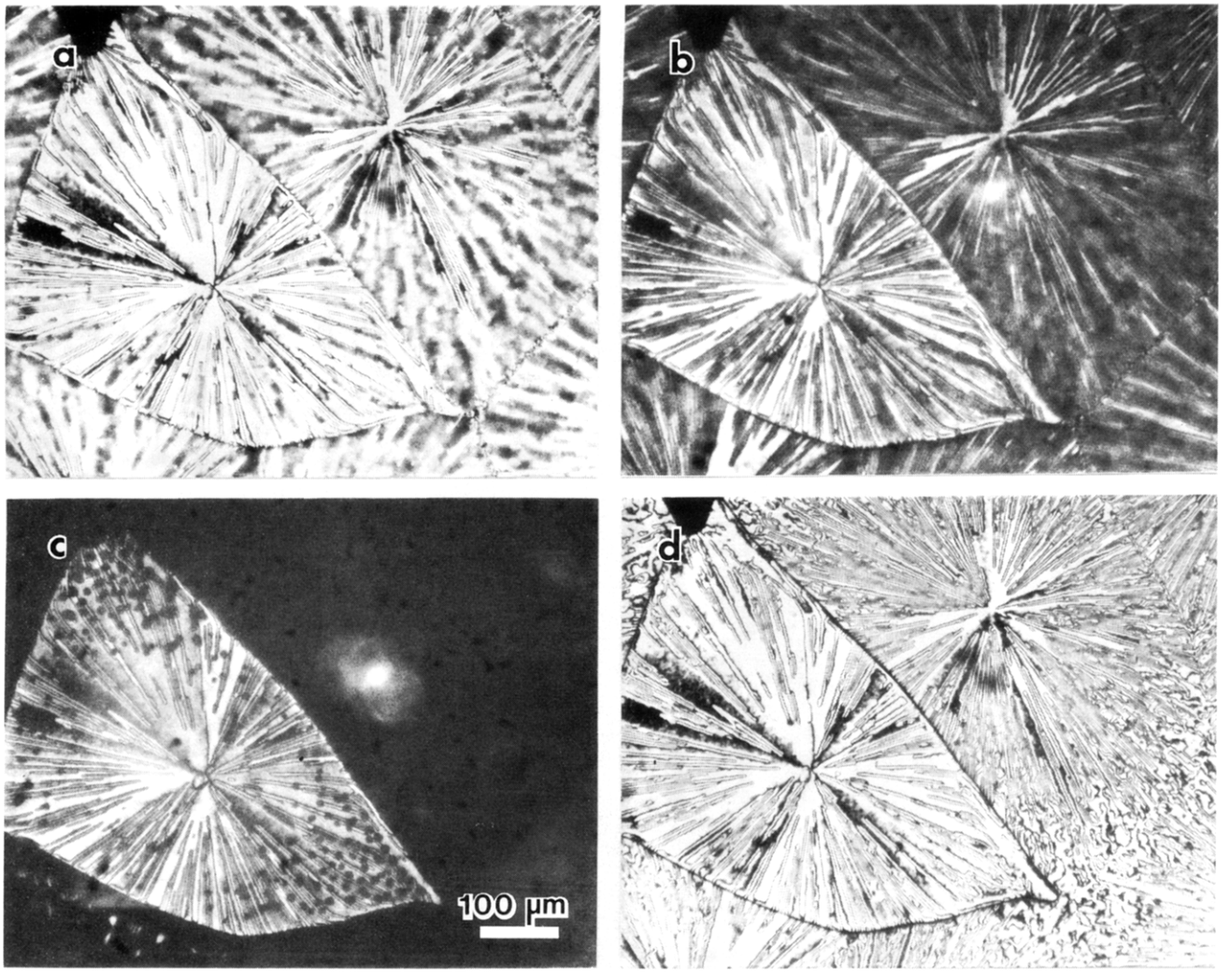

Figure 16. Typical effects of heating and cooling on the morphology of a 25:75 E7:NOA65 that had been UV-irradiated with 4.5 J/cm^2 at 40 °C. (a) Original morphology at 27 °C; (b) heated to 59.5 °C; (c) heated to 60.6 °C; (d) cooled to 37 °C.

LC droplets have been extracted shows wide departures from sphericity, widespread occurrence of fused or satellite droplets, and a bimodal size distribution. Minimal curing (only 0.04 J/cm^2) is needed to induce phase separation of LC from the polymer matrix; the resulting LC phase keeps increasing in the absence of further irradiation, mostly by nucleation of new droplets and less by growth.

The spherulitic-type morphology has a number of exceptional features. The nematic spherulites originate at a central $s = +1$ disclination line, grow through tangential accretion of the LC molecules, and are characterized by radially oriented defects. We have identified these defects as surface inversion walls, which can be initiated by a variety of factors, both inherent to the spherulite and external (surface influences, local compositional fluctuations). We found that these inversion walls are systematically initiated by $s = +1/2$ disclination lines (and terminated by $s = -1/2$ counterparts); at interspherulitic boundaries they are reoriented parallel to the perimeter even though their constituent molecular orientation remains the same. The spherulites as well as most of the inversion walls (with the exception of those at the periphery) survive intact after heating to significantly above the nematic–isotropic transition temperature.

Acknowledgment. We are grateful to Dr. P. E. Cladis for helpful discussions.